HHS Public Access

Author manuscript

Free Radic Biol Med. Author manuscript; available in PMC 2019 February 01.

Published in final edited form as:

Free Radic Biol Med. 2018 February 01; 115: 179–190. doi:10.1016/j.freeradbiomed.2017.11.025.

Crosstalk between autophagy and oxidative stress regulates proteolysis in the diaphragm during mechanical ventilation

Ashley J. Smuder[a], **Kurt J. Sollanek**[b], **W. Bradley Nelson**[c], **Kisuk Min**[d], **Erin E. Talbert**[e], **Andreas N. Kavazis**[f], **Matthew B. Hudson**[g], **Marco Sandri**[h], **Hazel H. Szeto**[i], and **Scott K. Powers**[j]

[a]Department of Exercise Science, University of South Carolina, Columbia, SC 29208

[b]Department of Kinesiology, Sonoma State University, Rohnert Park, CA 94928

[c]Department of Natural Sciences, Ohio Dominican University, Columbus, OH 43219

[d]Department of Pharmacology, Yale University, New Haven, CT 06520

[e]Department of Molecular Virology, Immunology and Medical Genetics, Ohio State University, Columbus, OH 43210

[f]School of Kinesiology, Auburn University, Auburn, AL 36849

[g]Department of Kinesiology and Applied Physiology, University of Delaware, Newark, DE 19716

[h]Department of Biomedical Science, University of Padova, Padova, Italy

[i]Department of Pharmacology, Weill Cornell Medical College, New York, NY 10021

[j]Department of Applied Physiology and Kinesiology, University of Florida, Gainesville, FL 32611

Abstract

Mechanical ventilation (MV) results in the rapid development of ventilator-induced diaphragm dysfunction (VIDD). While the mechanisms responsible for VIDD are not fully understood, recent data reveal that prolonged MV activates autophagy in the diaphragm, which may occur as a result of increased cellular reactive oxygen species (ROS) production. Therefore, we tested the hypothesis that 1) accelerated autophagy is a key contributor to VIDD; and that 2) oxidative stress is required to increase the expression of autophagy genes in the diaphragm. Our findings reveal that targeted inhibition of autophagy in the rat diaphragm prevented MV-induced muscle atrophy and contractile dysfunction. Attenuation of VIDD in these animals occurred as a result of increased diaphragm concentration of the antioxidant catalase and reduced mitochondrial ROS emission, which corresponded to reductions in the activity of calpain and caspase-3. To determine

Corresponding author and reprint requests: Ashley J. Smuder. Department of Exercise Science, University of South Carolina, Public Health Research Center, Room 227, 921 Assembly St, Columbia, SC 29208, Phone: (803) 777-2185. smuder@mailbox.sc.edu.

Disclosures

The SS peptides technology has been licensed for commercial development by the Cornell Research Foundation (CRF), and both CRF and Hazel H. Szeto have financial interests.

if increased ROS production is required for the upregulation of autophagy biomarkers in the diaphragm, rats that were administered the mitochondrial-targeted peptide SS-31 during MV. Results from this study demonstrated that mitochondrial ROS production in the diaphragm during MV is required for the increased expression of key autophagy genes (i.e. LC3, ATG7, ATG12, Beclin1 and p62), as well as for increased activity of cathepsin L. Together, these data reveal that autophagy is required for VIDD, and that autophagy inhibition reduces MV-induced diaphragm ROS production and prevents a positive feedback loop whereby increased autophagy is stimulated by oxidative stress, resulting in further increases in ROS and autophagy.

Graphical Abstract

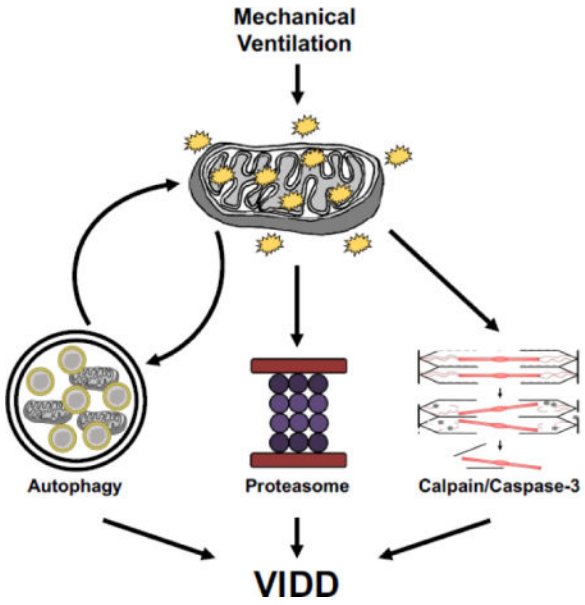

Keywords

diaphragm; autophagy; oxidative stress; respiratory; antioxidant; mitochondria

Introduction

Mechanical ventilation (MV) is used to maintain adequate alveolar ventilation in patients unable to maintain blood gas homeostasis with spontaneous breathing. While MV is a life-saving intervention for critically ill patients, prolonged MV results in the rapid development of diaphragm weakness due to both myofiber atrophy and contractile dysfunction; this condition is termed ventilator-induced diaphragm dysfunction (VIDD) [1–3]. VIDD is important because diaphragm weakness is predicted to contribute to difficulties in weaning patients from the ventilator [4–6]. Unfortunately, there is currently no standard therapy to prevent VIDD. Therefore, improving our understanding of the cellular processes that promote VIDD is essential to develop a therapeutic strategy to protect against MV-induced diaphragm weakness.

Although the molecular underpinnings that cause VIDD remain unclear, it is well established that prolonged MV results in accelerated proteolysis in the diaphragm [7]. Specifically, our laboratory has shown that MV-induced activation of calpain and the proteasome system in the diaphragm are associated with the breakdown of myofibrillar proteins [8–10], and caspase-3 activity is associated with both contractile protein cleavage and apoptosis [8, 11]. In addition to these proteolytic pathways, autophagy is also activated in the diaphragm of both rodents and humans during prolonged MV [12,13]. However, the role that autophagy plays in the development of VIDD remains unclear. In this regard, evidence suggests that increased autophagy can be a double-edged sword. In theory, accelerated autophagy could produce protective or deleterious effects on skeletal muscle depending on the conditions [14, 15]. For example, MV-induced accelerated autophagy could promote diaphragm atrophy by eliminating healthy organelles and cytosolic proteins from muscle fibers [16]. In contrast, MV-induced autophagy could be protective by removing damaged mitochondria and aggregated proteins within diaphragm myofibers [16, 17].

In addition to the downstream effects of accelerated autophagy on diaphragm muscle function, the upstream trigger promoting accelerated autophagy is unknown. In this regard, it has been demonstrated that MV-induced increases in ROS production in the diaphragm leads to activation of several proteases along with oxidative modification of muscle proteins making them more susceptible to degradation [18–21]. The degradation of both cytosolic and myofibrillar proteins is a multistep process that requires the cooperation of several proteolytic components including the calpain, caspase-3, ubiquitin-proteasome and autophagy/lysosomal proteolytic systems [18–21]. We have recently discovered that prevention of MV-induced increases in mitochondrial ROS emission is sufficient to prevent the activation of the calpain, caspase-3 and ubiquitin-proteasome proteolytic systems in the diaphragm during MV [22]. However, the role that mitochondrial ROS emission plays in activating the autophagy/lysosomal system in the diaphragm during prolonged MV remains unknown. Therefore, the goal of these experiments was twofold: 1) to determine the effects of accelerated autophagy on VIDD and; 2) to determine if MV-induced increases in mitochondrial ROS emission is required to increase the expression of autophagy biomarkers in the diaphragm. Specifically, we tested the hypothesis that accelerated autophagy is required for VIDD and that MV-induced increases in mitochondrial ROS emission promote autophagy gene expression and activate autophagy in the diaphragm.

Material and methods

Animals

Young adult (~6 month old) female Sprague-Dawley rats were used in these experiments. The Institutional Animal Care and Use Committee of the University of Florida approved these experiments.

Experimental Design

To investigate the role that autophagy plays in VIDD we performed two separate experiments.

Experiment 1—To test the hypothesis that increased autophagy is required for VIDD, we administered a dominant negative Atg5 (dnATG5) adeno-associated virus (AAV9) vector to the diaphragm to inhibit MV-induced autophagosome formation. Rats were randomly assigned to one of four experimental groups (n=10/group): 1) acutely anesthetized controls; animals treated with AAV9 expressing green fluorescent protein (GFP) (CON); 2) acutely anesthetized controls; animals treated with AAV9 expressing dnATG5-GFP (CON-dnATG5); 3) 12 hours of MV; animals treated with AAV9 expressing GFP (MV); and 4) 12 hours of MV; animals treated with AAV9 expressing dnATG5-GFP (MV-dnATG5). Primary dependent measures included the assessment of diaphragm cross-sectional area (CSA), contractile function, biomarkers of autophagy and biomarkers of oxidative stress.

Experiment 2—This experiment tested the hypothesis that increased mitochondrial ROS emission is required to promote autophagy gene expression and activate autophagy in the diaphragm of mechanically ventilated rats. Animals were assigned to one of three experimental groups (n=8/group): 1) an acutely anesthetized control group (CON); 2) a 12 hour MV group (MV); and 3) a 12 hour MV group treated with the mitochondria-targeted antioxidant SS-31 (MVSS). Dependent measures for experiment 2 included the assessment of biomarkers of autophagy including electron microscopy, western blot, real-time polymerase chain reaction and activity assays.

Experimental Protocol

Packaging and Purification of Recombinant AAV Vectors: The dnATG5 plasmid was a gift from Roberta Gottlieb (Addgene plasmid #13096). We constructed the pTRUF12-dnATG5 plasmid by PCR amplifying the dnATG5 sequence into the SpeI and ClaI sites of pTRUF12. Verification of the appropriate fusion sequence was performed by DNA sequencing at the University of Florida DNA Sequencing Core Facility. The GFP expressing empty vector, pTRUF12 was used as a control plasmid. The rAAV pTRUF12-dnATG5 and pTRUF12 were generated, purified and tittered at the University of Florida Gene Therapy Center Vector Core Lab as previously described [23]. The conjugation of ATG12 to ATG5 is a required step in the elongation of the autophagosome [24, 25]. This mutated form of ATG5 is defective in its conjugation to ATG12, which is required for LC3 incorporation into the early autophagosomal structure, and thus inhibits autophagy at the level of autophagosome formation. Western blots for GFP were performed to verify the presence of the constructs in all animals (data not shown).

Surgical Protocol for gene transduction: To prevent MV-induced autophagy in the diaphragm we delivered an AAV vector containing dnATG5 to the costal diaphragm via direct injection. This technique is described in recent reports [13, 26]. Importantly, this method of gene transfer has been shown to effectively transduce the rat diaphragm with no adverse side effects [13, 26]. Animals were studied four weeks after AAV injection.

SS-31 Administration: The mitochondria-targeted antioxidant SS-31 was dissolved in saline and delivered in a bolus (loading) dose (3 mg/kg, subcutaneous injection) 15 minutes before initiation of MV. A constant intravenous infusion (0.05 mg/kg/hr) of SS-31 was maintained throughout MV. Previous work demonstrated that this dose of SS-31 in spontaneous

breathing animals does not affect diaphragm CSA, force production or mitochondrial respiratory function [27]. In addition, we also determined that SS-31 administration in mechanically ventilated animals is sufficient to prevent diaphragm atrophy, contractile dysfunction, mitochondrial dysfunction and ROS production [27].

Mechanical Ventilation: Control animals were not exposed to MV and were acutely anesthetized with sodium pentobarbital (60 mg/kg body weight intraperitoneally). MV animals were tracheostomized and mechanically ventilated with a pressure-controlled ventilator (Servo Ventilator 300, Siemens) for 12 hours as previously reported [28]. The carotid artery was cannulated to permit the continuous measurement of blood pressure during the protocol. A venous catheter was inserted into the jugular vein for continuous infusion of sodium pentobarbital (~10 mg/kg/hr) and fluid replacement. Body temperature was maintained at ~37°C by use of a heating blanket and heart rate was monitored via lead II electrocardiograph.

Systemic and Biological Response to MV: Prior to the initiation of MV, no significant differences existed in body weight between the experimental groups. Importantly, 12 hours of MV did not significantly alter body weight between groups ($p<0.05$). In addition, heart rate (HR), systolic blood pressure (SBP), arterial partial pressures of O_2 (PaO_2), CO_2 ($PaCO_2$) and pH were all maintained relatively constant during MV and no significant differences existed between groups (Table 1 and [27]). In addition, the colonic (body) temperature remained relatively constant (36°C-37°C) during MV. At the completion of the MV protocol, there was no visible indication of lung injury and no evidence of infection, indicating that our aseptic surgical technique was successful.

Biochemical Measures

Western Blot Analysis—Diaphragm protein extracts were assayed as previously described [29]. Briefly, diaphragm tissues were homogenized 1:10 (wt/vol) in 5 mM Tris (pH 7.5) and 5 mM EDTA (pH 8.0) with a protease inhibitor cocktail (Sigma-Aldrich, St. Louis, MO) and centrifuged at 1500 *g* for 10 min at 4°C. Supernatant was collected and protein content was assessed by the Bradford method (Sigma-Aldrich). Proteins were separated via polyacrylamide gel electrophoresis. Membranes were probed for Beclin 1 (#3495), Atg12 (#4180), LC3B (#2775) (Cell Signaling Technology, Danvers, MA), Atg7 (NBP2-24682) (Novus Biologicals, Minneapolis, MN), p62 (ab56416), catalase (ab16731), PMP70 (ab3421) (Abcam, Cambridge, UK) and cathepsin L (sc-6498), spectrin (sc-48382). α-tubulin (sc-58667) (Santa Cruz Biotechnology, Dallas, TX) was also probed for as a loading control. In addition, mitochondrial protein extracts were also assayed via western blot. Membranes were probed for 4-HNE (ab46545), Parkin (ab15954), PINK1 (ab23707), Mul1 (ab84067), p62 (ab56416) (Abcam), OPA1 (612606), DLP1 (611112) (BD Biosciences, San Jose, CA), Mfn2 (M6444) (Sigma-Aldrich) and Fis1 (alx-210-907) (Enzo Life Sciences, Farmingdale, NY). VDAC (sc-8829) (Santa Cruz) was also probed as a loading control for all mitochondrial proteins.

Real-time Polymerase Chain Reaction—Total RNA was isolated from diaphragm tissue with TRIzol Reagent (Life Technologies, Carlsbad, CA). Total RNA (5 μg) was then

reverse transcribed with the Superscript III First-Strand Synthesis System for RT-PCR (Life Technologies), using oligo(dT)20 primers. One microliter of cDNA was added to a 25 μl PCR reaction for real-time PCR using Taqman chemistry and the ABI StepOnePlus Real-Time PCR system (ABI, Foster City, CA) as previously described [29]. *β-Glucuronidase* was chosen as the reference gene based on previous work showing unchanged expression with our experimental manipulations [30, 31]. mRNA transcripts were assayed using predesigned rat primer and probe sequences commercially available from Applied Biosystems (Assays-on-Demand).

Cathepsin L Activity—Diaphragm muscle was homogenized 1:5 (wt/vol) in ice cold CL Buffer (provided in the kit). Samples were centrifuged at 1500 *g* for 5 min at 4°C. Supernatant was collected and protein concentration was assayed via the Bradford method. Cathepsin L activity was measured fluorometrically according to the manufacturer's instructions (Abcam).

Measurement of *In Vitro* Diaphragmatic Contractile Properties—A muscle strip, including the tendinous attachments at the central tendon and rib cage was dissected from the midcostal region. The strip was suspended vertically between two lightweight Plexiglas clamps with one end connected to an isometric force transducer (model FT-03, Grass Instruments, Quincy, MA) within a jacketed tissue bath. The force output was recorded via a computerized data-acquisition system (Super Scope II, GW Instruments Somerville, MA). The muscle strip was stimulated along its entire length with platinum wire electrodes (modified S48 stimulator, Grass Instruments) by using supramaximal (~150%) stimulation voltage to determine the optimum contractile length (*Lo*). To measure maximal isometric twitch force each strip was stimulated supramaximally with 120-V pulses at 1 Hz and to measure the force frequency response each strip was stimulated supramaximally with 120-V pulses at 15– 160 Hz [32].

Mitochondrial respiration and ROS emission—Mitochondrial oxygen consumption and ROS emission were measured in isolated mitochondria from diaphragm muscle using previously described techniques [33]. Respiration was measured via polarography in water-jacketed respiration chambers maintained at 37°C (Hansatech Instruments, King's Lynn, UK). 5 mM pyruvate and 5 mM malate and 0.25 mM ADP were added to stimulate state 3 respiration. The RCR was calculated by dividing state 3 by state 4 respiration. Diaphragmatic mitochondrial ROS emission was determined using Amplex™ Red (Molecular Probes, Eugene, OR). Details of this assay have been described previously [33]. Mitochondrial ROS production was measured using the creatine kinase energy clamp technique to maintain respiration at steady state using previously described methods [34].

Histological Measures

Electron Microscopy—Diaphragm muscle was fixed in a 4% paraformaldehyde solution in PBS. Samples were treated and prepared for electron microscopy examination by the University of Florida ICBR Electron Microscopy Core Lab. A Hitachi H-7000 TEM was used to acquire diaphragm images.

Immunogold labeling of catalase—Diaphragm muscle was fixed in a 4% paraformaldehyde solution in PBS. Samples were treated and prepared for examination of immunogold labeling of catalase, and were analyzed by the University of Florida ICBR Electron Microscopy Core Lab. Anti-catalase antibody was obtained from Abcam (ab6573). A FEI Spirit TEM operated at 120kV was used to acquire diaphragm images.

Myofiber Cross-Sectional Area—Sections from frozen diaphragm samples were cut at 10 microns using a cryotome (Shandon Inc., Pittsburgh, PA) and stained for dystrophin, myosin heavy chain (MHC) type I and MHC type IIa proteins for fiber cross-sectional area analysis (CSA) as described previously [28]. Images were acquired via a monochrome camera attached to an inverted fluorescent microscope (Axiovert 200, Xeiss). Diaphragm myofiber CSA was determined using Scion software (NIH).

LC3 Immunohistochemistry—Sections from frozen diaphragm samples were cut at 10 microns using a cryotome. Diaphragm sections were blocked for an hour with 5% bovine serum albumin and 3% goat serum in PBS. LC3 primary (Cell Signaling Technology) and secondary (Alexa Fluro 488 goat anti-rabbit) reagents diluted in 1% bovine serum albumin [35]. Sections were mounted with vectashield mounting medium with dapi (Vector laboratories, Burlingame, CA). Images were acquired via a monochrome camera attached to an inverted fluorescent microscope (Axiovert 200, Xeiss).

Statistical Analysis: Comparisons between groups for each dependent variable were made by a one-way analysis of variance (ANOVA) and, when appropriate, a Tukey HSD (honestly significant difference) test was performed *post-hoc*. Significance was established at $p < 0.05$. Data are presented as means ± SEM. Statistical analysis was not performed on electron microscopy images due to the small sample size (n=2-4/group).

Results

dnATG5 diaphragm transduction ameliorates autophagic signaling

Preliminary studies were conducted to determine the appropriate administration of dnATG5 to reduce MV-induced autophagic signaling to basal levels. Our results confirm the effectiveness of our dosing protocol as MV resulted in a significant increase in the conjugation of Atg12-Atg5 (+188.5 ± 18.8 percent) and the activity of cathepsin L (+1.77 ± 0.24 fold), while MV animals that were administered dnATG5 showed no differences compared to CON animals (Figure 1A–B). In addition, we assessed the mRNA expression of several mitochondrial proteins required for the regulation of mitophagy in skeletal muscle. These data demonstrate that MV results in a significant increase in the mRNA expression of PINK1 (+2.67 ± 0.61 fold), p62 (+4.11 ± 0.61 fold), Mul1 (+4.16 ± 0.59 fold), Nix (+1.72 ± 0.24 fold) and BNIP3 (+1.43 ± 0.07 fold) (Figure 1C). In the diaphragm of MV-dnATG5 animals, PINK1, Nix and BNIP3 did not differ from CON animals; however, p62 (+2.63 ± 0.43 fold) and Mul1 (+2.53 ± 0.29 fold) remained elevated in these animals compared to CON. Finally, our results also indicate that MV and MV-dnATG5 had no effect on the expression of Parkin in the diaphragm compared to CON animals.

Inhibition of MV-induced autophagy ameliorates VIDD

Twelve hours of MV resulted in a reduction in diaphragm specific force production at all stimulation frequencies (15-160 Hz; −21.3 ± 1.60 percent) and decreased myofiber CSA (Type I −32.7 ± 6.71; IIa −30.7 ± 6.25; IIb/x −39.3 ± 4.64 percent) compared to CON. Importantly, dnATG5 transduction in the diaphragm prior to MV was sufficient to attenuate MV-induced diaphragm contractile dysfunction at stimulation frequencies greater than 15 Hz and also prevented the MV-induced reduction in diaphragm myofiber CSA (Figure 2A–B). In addition, no differences existed in diaphragm force production or muscle fiber size between CON and CON-dnATG5 animals.

Inhibition of autophagy prevents MV-induced autophagosome formation

Electron microscopy images were used to visualize changes in diaphragm ultrastructure and autophagosome formation. The representative images shown in Figure 3A–B illustrate that independent of MV, dnATG5 did not adversely affect the diaphragm. Specifically, these images show intact sarcomeres with no obvious abnormalities in the ultrastructure of the fibers. Figure 3C depicts sample diaphragm images from MV animals. In these images, autophagic vesicles are visible within the diaphragm. Finally, Figure 3D portrays images from MV-dnATG5 animals; importantly, images from these animals appear to contain relatively few autophagosomes.

Effects of dnATG5 on diaphragm proteolytic activity

Evidence in cardiomyocytes suggests that a regulatory cross-talk exists between autophagy and other proteolytic systems [36]. Our data confirm that MV results in a significant increase in the activity of calpain (+142.9 ± 11.8 percent) and caspase-3 (+155.4 ± 10.5 percent), represented by the accumulation of the 145 kDa and 120 kDa breakdown products of spectrin, respectively (Figure 4A–B). In addition, prevention of increased autophagy in the diaphragm prevents the MV-induced activation of caspase-3. Our findings also confirm previous reports that prolonged MV results in increased mRNA expression of the muscle-specific E3 ligases MuRF1 (+9.34 ± 2.21 fold) and Atrogin-1/MaFbx (+4.83 ± 0.55 fold) in the diaphragm [10, 13, 37]. Note that dnATG5 diaphragm transduction did not influence the impact of prolonged MV on diaphragmatic expression of these E3 ligases (Figure 4C–D). In addition, prolonged MV resulted in significant increases in diaphragm mRNA expression of polyubiquitin (pUB) (+2.06 ± 0.29 fold) and the proteasome regulatory complex p28α (+1.79 ± 0.11 fold); these effects were also not impacted by transduction of dnATG5 in the diaphragm (Figure 4E–F).

Prevention of accelerated autophagy prevents MV-induced mitochondrial dysfunction and oxidative stress—The current study shows that MV results in increased diaphragm mitochondrial ROS emission (state 3: +1.64 ± 0.16 fold; state 4: +1.79 ± 0.19 fold) and a reduced respiratory control ratio (RCR) (−0.56 ± 0.02 fold) compared to CON animals (Figure 5A–C). Reduced RCR in MV animals primarily occurred as a result of an increase in state 4 oxygen consumption (+1.24 ± 0.04 fold), as no significant differences existed in state 3 respiration between groups. Importantly, our results also confirm that inhibition of autophagy in control animals did not impact mitochondrial function, as no

differences existed between the CON and CON-dnATG5 groups in RCR or ROS emission. Importantly, animals in the MV-dnATG5 group were rescued from the MV-induced changes to these markers of oxidative stress and mitochondrial damage.

The mechanism(s) to explain the protection against MV-induced oxidative stress in animals treated with the dnATG5 is unclear but could be linked the fact that accelerated autophagy has been shown to reduce cellular antioxidant capacity by autophagic removal of peroxisomes and a subsequent reduction in catalase [38]. Our data reveal that compared to both CON and dnATG5 animals, prolonged MV results in a significant reduction in catalase protein abundance in the diaphragm (−21.5 ± 8.12 percent), while no differences in catalase mRNA expression exist between groups (Figure 6A–B). To determine the effect of autophagy inhibition on peroxisome content, we measured the peroxisome membrane protein 70 (PMP70). Animals in the MV-dnATG5 group demonstrated a significant increase (+156.7 ± 22.4 percent) in PMP70 compared to all other groups (Figure 6C). Finally, immunogold labeling of catalase in the diaphragm was used to observe differences in catalase within the diaphragm muscle. Visual assessment of these images reveals a greater abundance of catalase in CON and MV animals treated with dnATG5 compared to MV animals (Figure 6D).

The mitochondrial peptide SS-31 reduces MV-induced autophagosome formation and preserves diaphragm morphology

Electron microscopy images were obtained to visualize alterations to diaphragm muscle fiber ultrastructure that occur as a result of prolonged MV. Figure 7A depicts differences in the abundance of autophagic vacuoles between CON, MV and MVSS animals, while Figure 7B and 7C images demonstrate differences between mitochondrial structure between the two groups, with MV resulting in the appearance of rounded mitochondria with a loss of cristae structure, which may be indicative of compromised mitochondrial function.

Delivery of a mitochondrial-targeted peptide (SS-31) prevents MV-induced biomarkers of autophagy in the diaphragm

Prolonged MV results in increased mRNA and protein expression of LC3 (+1.82 ± 0.30 fold), Atg7 (+2.16 ± 0.07 fold), Atg12 (+1.92 ± 0.29 fold), Beclin 1 (+1.91 ± 0.30 fold) and p62 (+2.23 ± 0.34 fold) in the diaphragm compared to CON, which is attenuated in animals treated with SS-31 (Figure 8A). In addition, MV results in the appearance of LC3 punctae in diaphragm muscle fibers (+26.9 ± 3.10 fold), and administration of SS-31 to mechanically ventilated animals was sufficient to diminish the formation of LC3 punctae (Figure 8B). Finally, assessment of the expression of cathepsin B, D and L in the diaphragm revealed an increase in mRNA expression of cathepsin B (+2.64 ± 0.27 fold) and cathepsin L (+8.44 ± 1.56 fold) in animals exposed to prolonged MV, which was attenuated in MVSS animals (Figure 8C). In addition, following prolonged MV there was a significant increase in the activity of cathepsin L in the diaphragm (+202.3 ± 35.15 percent) compared to CON, which was prevented by treating animals with SS-31 (Figure 8D).

Discussion

Inhibition of MV-induced autophagy prevents VIDD

Autophagy is a catabolic process that involves lysosomal degradation of cytosolic proteins and organelles. In general, autophagy occurs on a continuous basis at low levels in muscle tissue and is important for maintaining the breakdown of dysfunctional cytosolic material [39, 40]. Specifically, studies show that basal levels of autophagy are required for normal muscle function, and that deletion of specific autophagy genes can result in significant functional deficits [41, 42]. However, under pathological conditions autophagy can be greatly increased to promote a deleterious rate of protein removal. Indeed, pathologically high levels of autophagy can result in the elimination of vital cellular organelles and proteins, and potential cross-talk between other proteolytic systems to increase cell death and promote muscle atrophy [43]. In this regard, MV results in increased autophagosome formation and increased expression of autophagy-related genes in the diaphragm, and is associated with muscle weakness [13]. Indeed, our data confirm that autophagy is required for VIDD, as inhibition of autophagy was sufficient to prevent diaphragm muscle atrophy and contractile dysfunction in rats after 12 hours of MV.

Effects of autophagy inhibition on diaphragm proteolysis

The autophagy/lysosomal system has been shown to participate in cross-talk with the calpain, caspase-3 and proteasome degradation pathways [44–47]. Specifically, calpain activation can act as a negative regulator of autophagy by cleaving Atg5 and preventing the conjugation of Atg5-Atg12 [44, 45, 48]. In addition, caspase-3 activity may also play a role as a negative regulator of autophagy by shifting the signaling of Beclin-1 from autophagic protein degradation to apoptotic protein degradation [46, 49]. Independent of these potential mechanisms, our laboratory has established that increased diaphragm ROS production is an essential upstream trigger to activate both the calpain and caspase-3 proteolytic systems [50]. Moreover, oxidative modification of myofibrillar proteins increases their susceptibility to degradation by calpain and caspase-3, which promotes increased proteolysis and skeletal muscle dysfunction [9]. Therefore, inhibiting autophagy may prevent calpain and caspase-3-dependent proteolysis via the reduction in oxidative damage to the diaphragm. Our data supports this hypothesis as autophagy inhibition downregulated calpain and caspase-3 activity rather that increasing it.

In contrast to the finding that inhibition of autophagy blunted the MV-induced activation of both calpain and caspase-3 in the diaphragm, our results reveal that biomarkers of the proteasome system remained elevated in the diaphragms of MV- dnATG5 animals. This observation is comparable to previous reports indicating that pharmacological inhibition of autophagy does not prevent increased proteasome activity in the heart [47, 51]. This finding is consistent with the concept that, in the absence of accelerated autophagy, the proteasome system is upregulated in a compensatory manner to degrade damaged proteins in the diaphragm during MV. Finally, while evidence from our lab has shown that calpain and caspase-3 activity are required for VIDD [8], we have also demonstrated that the ubiquitin proteasome system does not significantly contribute to MV-induced diaphragm weakness

[10]. Based on this previous report and the current findings, activation of the ubiquitin proteasome system when autophagy is inhibited should not affect the diaphragm during MV.

Mitochondrial ROS emission promotes autophagosome formation in the diaphragm

The autophagy/lysosomal system is activated in numerous conditions that promote muscle wasting (i.e. denervation, hind-limb immobilization, chemotherapy etc.) [14, 15]. During each of these conditions, increased generation of ROS results in oxidative stress and organelle damage within skeletal muscle myofibers [52]. Moreover, increased cellular ROS production results in the increased expression of autophagy-related genes and the activation of autophagy [53–55]. While basal autophagy is necessary for cell survival, excessive autophagy is associated with muscle atrophy [56–58]. In reference to VIDD, it is established that prolonged ventilator support results in increased ROS production in the diaphragm along with increased expression of autophagy genes [12, 27, 29, 33, 59]. The current study provides evidence that MV-induced mitochondrial ROS production is a requirement for the MV-induced increase in the expression of key autophagy proteins in the diaphragm. Indeed, administration of the mitochondrial-targeted antioxidant peptide SS-31 prevented both the MV-induced expression of specific biomarkers of autophagy and the increase in autophagosome formation within the diaphragm. Coupled with our previous work, these findings establish a significant role for MV-induced mitochondrial ROS production in the regulation of four key proteolytic pathways (e.g. calpain, caspase-3, proteasome and autophagy) in the diaphragm during prolonged MV.

MV-induced autophagy is required for diaphragm mitochondrial dysfunction and oxidative stress

Paradoxical to our finding that prevention of MV-induced increases in mitochondrial ROS production (via the antioxidant peptide SS-31) is sufficient to prevent MV-induced increases in biomarkers of autophagy in the diaphragm, our data also reveal that selective inhibition of autophagy via dnATG5 prevents both MV-induced mitochondrial ROS emission and oxidative stress. These results suggest that a regulatory cross-talk exists between oxidative stress and autophagy, whereby increased autophagy is stimulated by oxidative stress, resulting in further increases in both ROS production and autophagy. In this regard, similar results have been reported in other cell types when autophagy is inhibited [38, 60]. Specifically, it has been predicted that autophagy upregulation results in the selective degradation of the endogenous antioxidant catalase via elimination of peroxisomes and mitochondria, causing an increase in cellular ROS [38]. Therefore, autophagy inhibition may reduce ROS production and prevent a positive-feedback loop where increased autophagy is stimulated by oxidative stress, resulting in further increases in ROS and autophagy. Our results corroborate this finding as inhibiting autophagy prevented the degradation of catalase and resulted in increased expression of PMP70 within the diaphragm.

Conclusions

In summary, these experiments provide the first evidence that autophagy plays a required role in the development VIDD. Further, our work reveals a novel cross-talk between autophagy and oxidative stress. These studies provide further insight into the mechanisms

responsible for VIDD and demonstrate the use of mitochondrial-targeted antioxidants as a potential therapy to prevent MV-induced diaphragm proteolysis.

Acknowledgments

This work was supported by the National Institutes of Health [Grant number R21AR064956].

Abbreviations

MV	mechanical ventilation
VIDD	ventilator-induced diaphragm dysfunction
pUB	polyubiquitin
dnATG5	dominant negative ATG5
SBP	systolic blood pressure
PaO_2	arterial partial pressures of O_2
$PaCO_2$	arterial partial pressures of CO_2

References

1. Levine S, Nguyen T, Taylor N, Friscia ME, Budak MT, Rothenberg P, Zhu J, Sachdeva R, Sonnad S, Kaiser LR, Rubinstein NA, Powers SK, Shrager JB. Rapid disuse atrophy of diaphragm fibers in mechanically ventilated humans. N Engl J Med. 2008; 358(13):1327–35. [PubMed: 18367735]
2. Powers SK, Shanely RA, Coombes JS, Koesterer TJ, McKenzie M, Van Gammeren D, Cicale M, Dodd SL. Mechanical ventilation results in progressive contractile dysfunction in the diaphragm. J Appl Physiol (1985). 2002; 92(5):1851–8. [PubMed: 11960933]
3. Shanely RA, Zergeroglu MA, Lennon SL, Sugiura T, Yimlamai T, Enns D, Belcastro A, Powers SK. Mechanical ventilation-induced diaphragmatic atrophy is associated with oxidative injury and increased proteolytic activity. Am J Respir Crit Care Med. 2002; 166(10):1369–74. [PubMed: 12421745]
4. Carlucci A, Ceriana P, Prinianakis G, Fanfulla F, Colombo R, Nava S. Determinants of weaning success in patients with prolonged mechanical ventilation. Crit Care. 2009; 13(3):R97. [PubMed: 19549301]
5. Petrof BJ, Jaber S, Matecki S. Ventilator-induced diaphragmatic dysfunction. Curr Opin Crit Care. 2010; 16(1):19–25. [PubMed: 19935062]
6. Laghi F, Cattapan SE, Jubran A, Parthasarathy S, Warshawsky P, Choi YS, Tobin MJ. Is weaning failure caused by low-frequency fatigue of the diaphragm? Am J Respir Crit Care Med. 2003; 167(2):120–7. [PubMed: 12411288]
7. Powers SK, Wiggs MP, Sollanek KJ, Smuder AJ. Ventilator-induced diaphragm dysfunction: cause and effect. Am J Physiol Regul Integr Comp Physiol. 2013; 305(5):R464–77. [PubMed: 23842681]
8. Nelson WB, Smuder AJ, Hudson MB, Talbert EE, Powers SK. Cross-talk between the calpain and caspase-3 proteolytic systems in the diaphragm during prolonged mechanical ventilation. Crit Care Med. 2012; 40(6):1857–63. [PubMed: 22487998]
9. Smuder AJ, Kavazis AN, Hudson MB, Nelson WB, Powers SK. Oxidation enhances myofibrillar protein degradation via calpain and caspase-3. Free Radic Biol Med. 2010; 49(7):1152–60. [PubMed: 20600829]
10. Smuder AJ, Nelson WB, Hudson MB, Kavazis AN, Powers SK. Inhibition of the ubiquitin-proteasome pathway does not protect against ventilator-induced accelerated proteolysis or atrophy in the diaphragm. Anesthesiology. 2014; 121(1):115–26. [PubMed: 24681580]

11. McClung JM, Kavazis AN, DeRuisseau KC, Falk DJ, Deering MA, Lee Y, Sugiura T, Powers SK. Caspase-3 regulation of diaphragm myonuclear domain during mechanical ventilation-induced atrophy. Am J Respir Crit Care Med. 2007; 175(2):150–9. [PubMed: 17082496]
12. Hussain SN, Mofarrahi M, Sigala I, Kim HC, Vassilakopoulos T, Maltais F, Bellenis I, Chaturvedi R, Gottfried SB, Metrakos P, Danialou G, Matecki S, Jaber S, Petrof BJ, Goldberg P. Mechanical ventilation-induced diaphragm disuse in humans triggers autophagy. Am J Respir Crit Care Med. 2010; 182(11):1377–86. [PubMed: 20639440]
13. Smuder AJ, Sollanek KJ, Min K, Nelson WB, Powers SK. Inhibition of forkhead boxO-specific transcription prevents mechanical ventilation-induced diaphragm dysfunction. Crit Care Med. 2015; 43(5):e133–42. [PubMed: 25746508]
14. Sandri M. Protein breakdown in muscle wasting: Role of autophagy-lysosome and ubiquitin-proteasome. Int J Biochem Cell Biol. 2013; 45(10):2121–9. [PubMed: 23665154]
15. Sandri M. Autophagy in skeletal muscle. FEBS Lett. 2010; 584(7):1411–6. [PubMed: 20132819]
16. Sandri M. Autophagy in health and disease. 3. Involvement of autophagy in muscle atrophy. Am J Physiol Cell Physiol. 2010; 298(6):C1291–7. [PubMed: 20089936]
17. Powers SK, Smuder AJ, Criswell DS. Mechanistic Links Between Oxidative Stress and Disuse Muscle Atrophy. Antioxid Redox Signal. 2011
18. Powers SK, Kavazis AN, DeRuisseau KC. Mechanisms of disuse muscle atrophy: role of oxidative stress. Am J Physiol Regul Integr Comp Physiol. 2005; 288(2):R337–44. [PubMed: 15637170]
19. Hasselgren PO, Fischer JE. Muscle cachexia: current concepts of intracellular mechanisms and molecular regulation. Ann Surg. 2001; 233(1):9–17. [PubMed: 11141219]
20. Jackman RW, Kandarian SC. The molecular basis of skeletal muscle atrophy. Am J Physiol Cell Physiol. 2004; 287(4):C834–43. [PubMed: 15355854]
21. Kandarian SC, Stevenson EJ. Molecular events in skeletal muscle during disuse atrophy. Exerc Sport Sci Rev. 2002; 30(3):111–6. [PubMed: 12150569]
22. Powers SK, Hudson MB, Nelson WB, Talbert EE, Min K, Szeto HH, Kavazis AN, Smuder AJ. Mitochondria-targeted antioxidants protect against mechanical-ventilation-induced diaphragm weakness. Crit Care Med.
23. Zolotukhin S, Potter M, Zolotukhin I, Sakai Y, Loiler S, Fraites TJ Jr, Chiodo VA, Phillipsberg T, Muzyczka N, Hauswirth WW, Flotte TR, Byrne BJ, Snyder RO. Production and purification of serotype 1, 2, and 5 recombinant adeno-associated viral vectors. Methods. 2002; 28(2):158–67. [PubMed: 12413414]
24. Gustafsson AB, Gottlieb RA. Recycle or die: the role of autophagy in cardioprotection. J Mol Cell Cardiol. 2008; 44(4):654–61. [PubMed: 18353358]
25. Shintani T, Mizushima N, Ogawa Y, Matsuura A, Noda T, Ohsumi Y. Apg10p, a novel protein-conjugating enzyme essential for autophagy in yeast. EMBO J. 1999; 18(19):5234–41. [PubMed: 10508157]
26. Smuder AJ, Falk DJ, Sollanek KJ, Nelson WB, Powers SK. Delivery of recombinant adeno-associated virus vectors to rat diaphragm muscle via direct intramuscular injection. Hum Gene Ther Methods. 2013; 24(6):364–71. [PubMed: 24006956]
27. Powers SK, Hudson MB, Nelson WB, Talbert EE, Min K, Szeto HH, Kavazis AN, Smuder AJ. Mitochondria-targeted antioxidants protect against mechanical ventilation-induced diaphragm weakness. Crit Care Med. 2011; 39(7):1749–59. [PubMed: 21460706]
28. Whidden MA, Smuder AJ, Wu M, Hudson MB, Nelson WB, Powers SK. Oxidative stress is required for mechanical ventilation-induced protease activation in the diaphragm. J Appl Physiol. 2010; 108(5):1376–82. [PubMed: 20203072]
29. Smuder AJ, Hudson MB, Nelson WB, Kavazis AN, Powers SK. Nuclear factor-kappaB signaling contributes to mechanical ventilation-induced diaphragm weakness*. Crit Care Med. 2012; 40(3): 927–34. [PubMed: 22080641]
30. DeRuisseau KC, Shanely RA, Akunuri N, Hamilton MT, Van Gammeren D, Zergeroglu AM, McKenzie M, Powers SK. Diaphragm unloading via controlled mechanical ventilation alters the gene expression profile. Am J Respir Crit Care Med. 2005; 172(10):1267–75. [PubMed: 16126937]

31. Deruisseau KC, Kavazis AN, Powers SK. Selective downregulation of ubiquitin conjugation cascade mRNA occurs in the senescent rat soleus muscle. Exp Gerontol. 2005; 40(6):526–31. [PubMed: 15963672]
32. Reid MB. Free radicals and muscle fatigue: Of ROS, canaries, and the IOC. Free Radic Biol Med. 2008; 44(2):169–79. [PubMed: 18191753]
33. Kavazis AN, Talbert EE, Smuder AJ, Hudson MB, Nelson WB, Powers SK. Mechanical ventilation induces diaphragmatic mitochondrial dysfunction and increased oxidant production. Free Radic Biol Med. 2009; 46(6):842–50. [PubMed: 19185055]
34. Messer JI, Jackman MR, Willis WT. Pyruvate and citric acid cycle carbon requirements in isolated skeletal muscle mitochondria. Am J Physiol Cell Physiol. 2004; 286(3):C565–72. [PubMed: 14602577]
35. Smuder AJ, Kavazis AN, Min K, Powers SK. Doxorubicin-induced markers of myocardial autophagic signaling in sedentary and exercise trained animals. J Appl Physiol (1985). 2013; 115(2):176–85. [PubMed: 23703114]
36. Yamaguchi O, Taneike M, Otsu K. Cooperation between proteolytic systems in cardiomyocyte recycling. Cardiovasc Res. 2012; 96(1):46–52. [PubMed: 22843702]
37. Smuder AJ, Min K, Hudson MB, Kavazis AN, Kwon OS, Nelson WB, Powers SK. Endurance exercise attenuates ventilator-induced diaphragm dysfunction. J Appl Physiol (1985). 2012; 112(3):501–10. [PubMed: 22074717]
38. Yu L, Wan F, Dutta S, Welsh S, Liu Z, Freundt E, Baehrecke EH, Lenardo M. Autophagic programmed cell death by selective catalase degradation. Proc Natl Acad Sci U S A. 2006; 103(13):4952–7. [PubMed: 16547133]
39. Zhang YW, Shi J, Li YJ, Wei L. Cardiomyocyte death in doxorubicin-induced cardiotoxicity. Arch Immunol Ther Exp (Warsz). 2009; 57(6):435–45. [PubMed: 19866340]
40. Hamacher-Brady A, Brady NR, Gottlieb RA. Enhancing macroautophagy protects against ischemia/reperfusion injury in cardiac myocytes. J Biol Chem. 2006; 281(40):29776–87. [PubMed: 16882669]
41. Nakai A, Yamaguchi O, Takeda T, Higuchi Y, Hikoso S, Taniike M, Omiya S, Mizote I, Matsumura Y, Asahi M, Nishida K, Hori M, Mizushima N, Otsu K. The role of autophagy in cardiomyocytes in the basal state and in response to hemodynamic stress. Nat Med. 2007; 13(5): 619–24. [PubMed: 17450150]
42. Portbury AL, Willis MS, Patterson C. Tearin' up my heart: proteolysis in the cardiac sarcomere. J Biol Chem. 2011; 286(12):9929–34. [PubMed: 21257759]
43. Sciarretta S, Hariharan N, Monden Y, Zablocki D, Sadoshima J. Is autophagy in response to ischemia and reperfusion protective or detrimental for the heart? Pediatric cardiology. 2011; 32(3): 275–81. [PubMed: 21170742]
44. Yousefi S, Perozzo R, Schmid I, Ziemiecki A, Schaffner T, Scapozza L, Brunner T, Simon HU. Calpain-mediated cleavage of Atg5 switches autophagy to apoptosis. Nat Cell Biol. 2006; 8(10): 1124–32. [PubMed: 16998475]
45. Liang C. Negative regulation of autophagy. Cell Death Differ. 2010; 17(12):1807–15. [PubMed: 20865012]
46. Djavaheri-Mergny M, Maiuri MC, Kroemer G. Cross talk between apoptosis and autophagy by caspase-mediated cleavage of Beclin 1. Oncogene. 2010; 29(12):1717–9. [PubMed: 20101204]
47. Wang XJ, Yu J, Wong SH, Cheng AS, Chan FK, Ng SS, Cho CH, Sung JJ, Wu WK. A novel crosstalk between two major protein degradation systems: regulation of proteasomal activity by autophagy. Autophagy. 2013; 9(10):1500–8. [PubMed: 23934082]
48. Stefan MS, Shieh MS, Pekow PS, Rothberg MB, Steingrub JS, Lagu T, Lindenauer PK. Epidemiology and outcomes of acute respiratory failure in the United States, 2001 to 2009: a national survey. J Hosp Med. 2013; 8(2):76–82. [PubMed: 23335231]
49. Luo S, Rubinsztein DC. Apoptosis blocks Beclin 1-dependent autophagosome synthesis: an effect rescued by Bcl-xL. Cell Death Differ. 2010; 17(2):268–77. [PubMed: 19713971]
50. Powers SK, Kavazis AN, Levine S. Prolonged mechanical ventilation alters diaphragmatic structure and function. Crit Care Med. 2009; 37(10 Suppl):S347–53. [PubMed: 20046120]

51. Wang C, Wang X. The interplay between autophagy and the ubiquitin-proteasome system in cardiac proteotoxicity. Biochim Biophys Acta. 2015; 1852(2):188–94. [PubMed: 25092168]

52. Kiffin R, Bandyopadhyay U, Cuervo AM. Oxidative stress and autophagy. Antioxid Redox Signal. 2006; 8(1–2):152–62. [PubMed: 16487049]

53. Scherz-Shouval R, Elazar Z. ROS, mitochondria and the regulation of autophagy. Trends in cell biology. 2007; 17(9):422–7. [PubMed: 17804237]

54. Scherz-Shouval R, Shvets E, Fass E, Shorer H, Gil L, Elazar Z. Reactive oxygen species are essential for autophagy and specifically regulate the activity of Atg4. The EMBO journal. 2007; 26(7):1749–60. [PubMed: 17347651]

55. Klionsky DJ. Autophagy: from phenomenology to molecular understanding in less than a decade. Nature reviews. 2007; 8(11):931–7.

56. Hussain SN, Mofarrahi M, Sigala I, Kim HC, Vassilakopoulos T, Maltais F, Bellenis I, Chaturvedi R, Gottfried SB, Metrakos P, Danialou G, Matecki S, Jaber S, Petrof BJ, Goldberg P. Mechanical ventilation-induced diaphragm disuse in humans triggers autophagy. Am J Respir Crit Care Med. 182(11):1377–86.

57. Mammucari C, Milan G, Romanello V, Masiero E, Rudolf R, Del Piccolo P, Burden SJ, Di Lisi R, Sandri C, Zhao J, Goldberg AL, Schiaffino S, Sandri M. FoxO3 controls autophagy in skeletal muscle in vivo. Cell Metab. 2007; 6(6):458–71. [PubMed: 18054315]

58. O'Leary MF, Hood DA. Denervation-induced oxidative stress and autophagy signaling in muscle. Autophagy. 2009; 5(2):230–1. [PubMed: 19098460]

59. Smuder AJ, Gonzalez-Rothi EJ, Kwon OS, Morton AB, Sollanek KK, Powers SK, Fuller DD. Cervical spinal cord injury exacerbates ventilator-induced diaphragm dysfunction. J Appl Physiol (1985). 2015 jap 00488 2015.

60. Hollomon MG, Gordon N, Santiago-O'Farrill JM, Kleinerman ES. Knockdown of autophagy-related protein 5, ATG5, decreases oxidative stress and has an opposing effect on camptothecin-induced cytotoxicity in osteosarcoma cells. BMC Cancer. 2013; 13:500. [PubMed: 24160177]

Highlights

- Mechanical ventilation induces increased autophagic signaling and oxidative stress in the diaphragm.
- Inhibition of autophagy is sufficient to prevent ventilator-induced diaphragm dysfunction.
- Mechanical ventilation-induced autophagy is required for diaphragm mitochondrial dysfunction and oxidative stress
- Mitochondrial reactive oxygen species emission promotes autophagosome formation in the diaphragm

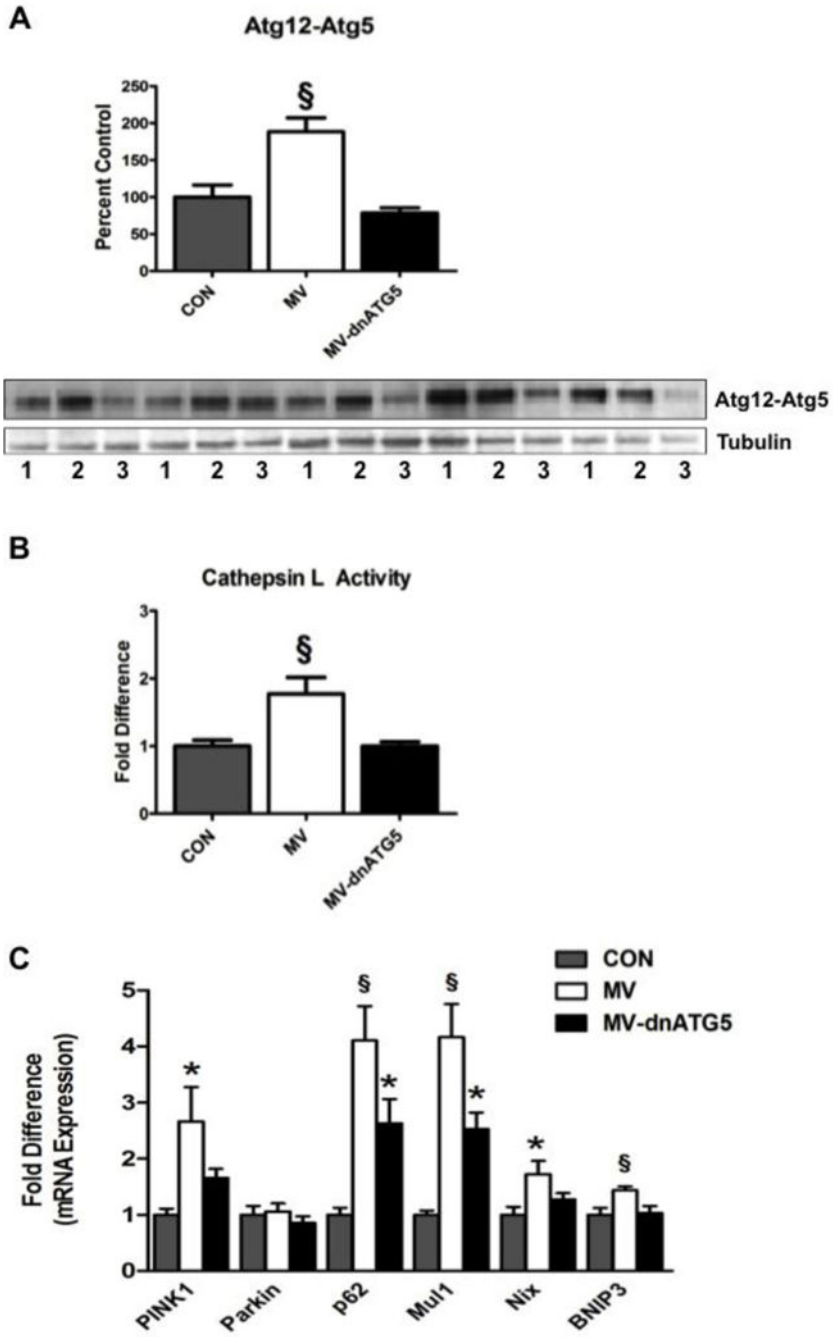

Figure 1.

Impact of MV on biomarkers of autophagy. **(A)** Atg12-Atg5 protein expression, **(B)** cathepsin L activity and **(C)** PINK1, parkin, p62, Mul1, Nix and BNIP3 mRNA expression in the diaphragm. Western blot images are shown below the graph. 1 = CON; 2 = MV; 3 = MV-dnATG5. Values are mean ± SEM. * Significantly different versus CON ($p<0.05$). § Significantly different versus all groups ($p<0.05$).

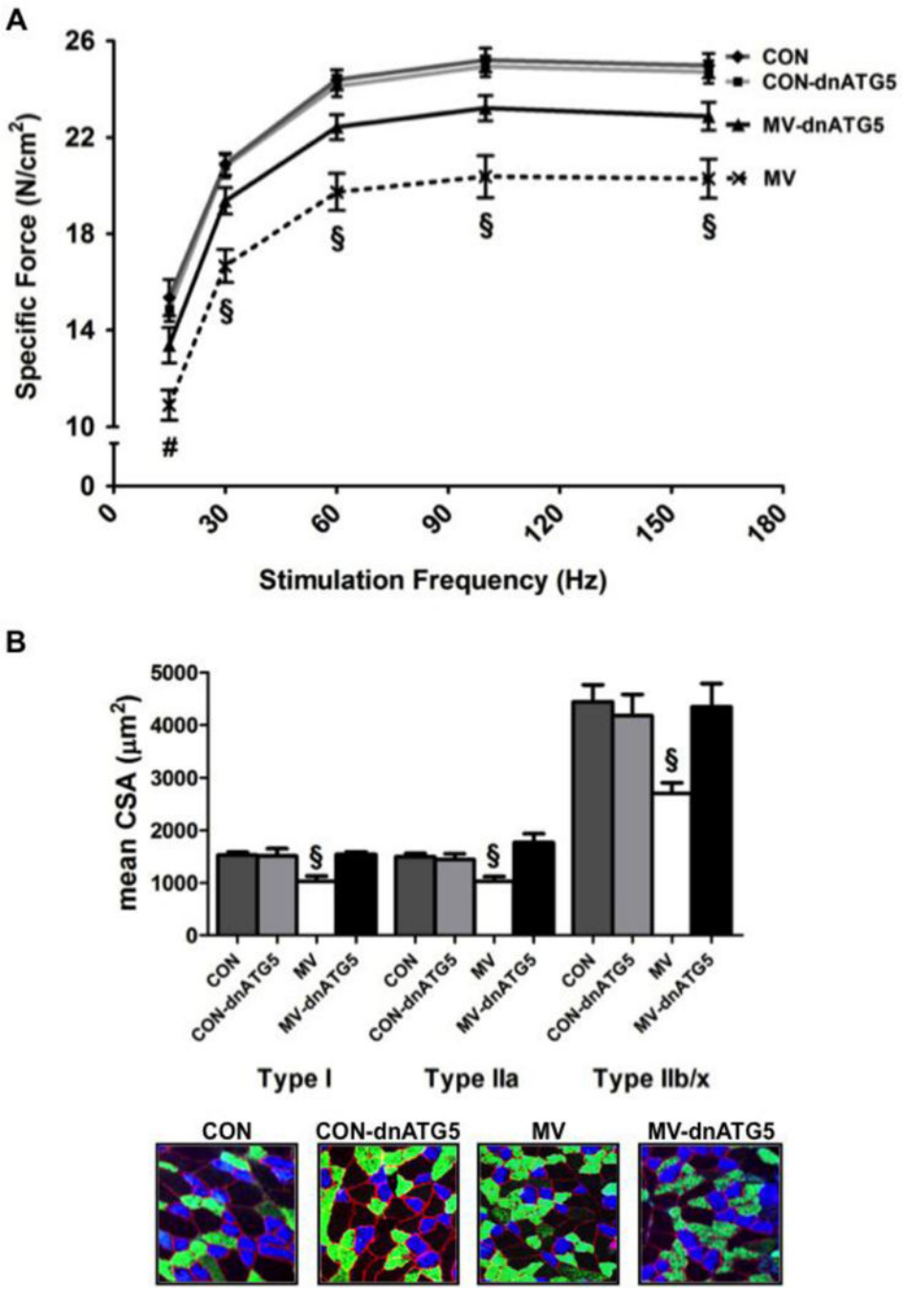

Figure 2.

(A) Diaphragm muscle force-frequency response. **(B)** Diaphragm muscle cross-sectional area in diaphragm skeletal muscle myofibers expressing myosin heavy chain (MHC) I (Type I), MHC IIa (Type IIa), and MHC IIb/IIx (Type IIb/IIx). Representative fluorescent staining of MHC I (DAPI filter/blue), MHC IIa (FITC filter/green), and dystrophin (Rhodamine filter/red) proteins in diaphragm samples are shown below the graph. Values are mean ± SEM. Groups represent: control GFP injected animals (CON), control dnATG5 injected animals (CON-dnATG5, MV GFP injected animals (MV) and MV dnATG5 injected animals

(MV-dnATG5). § Significantly different versus all groups ($p<0.05$). # Significantly different versus CON and CON-dnATG5 ($p<0.05$).

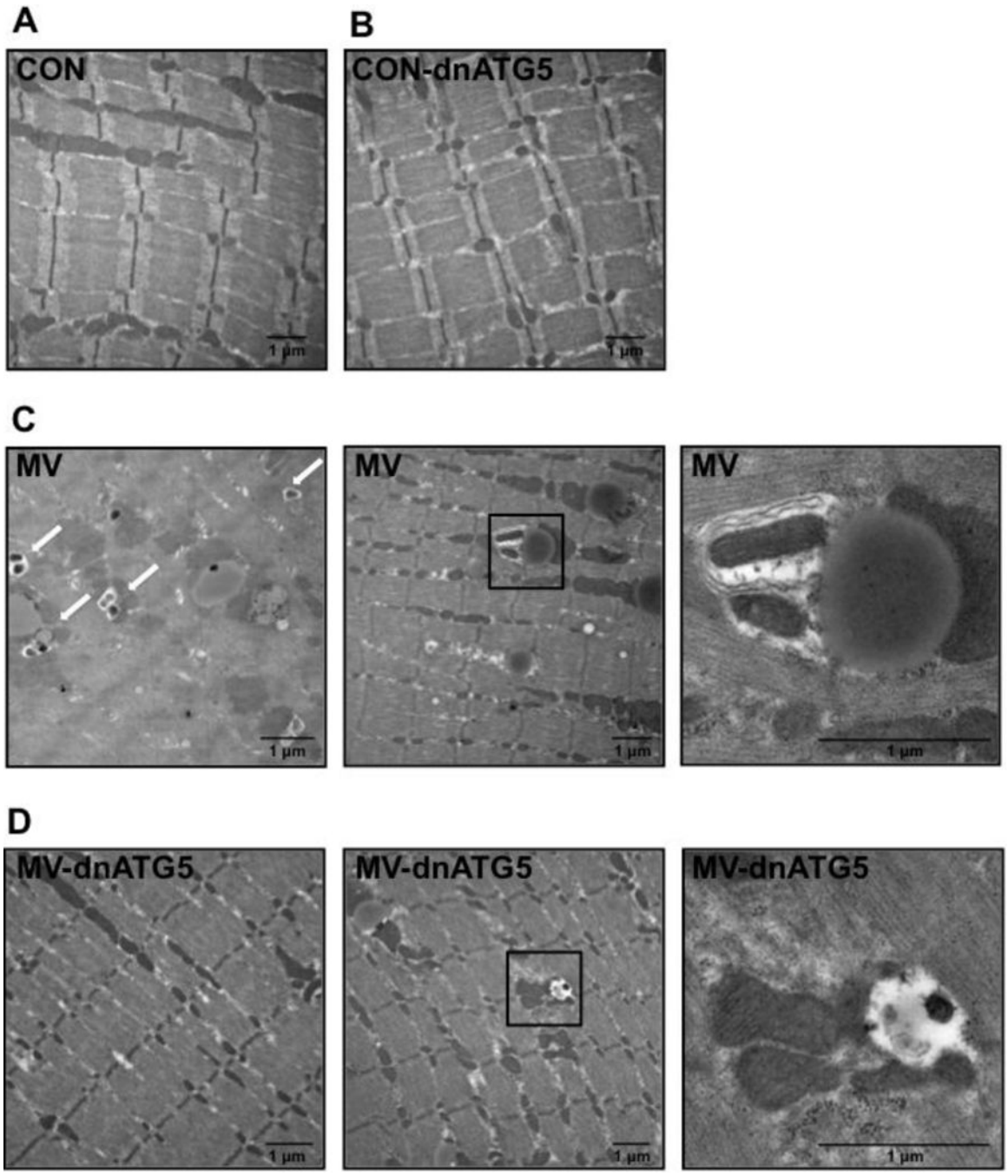

Figure 3.

Representative diaphragm muscle electron microscopy images for: **(A)** CON = control; non-ventilated, **(B)** CON-dnATG5 = control, non-ventilated, rAAV dnATG5, **(C)** MV = mechanically ventilated for 12 hours, and **(D)** MV-dnATG5 = mechanically ventilated; rAAV dnATG5. While arrows indicate autophagic vacuoles.

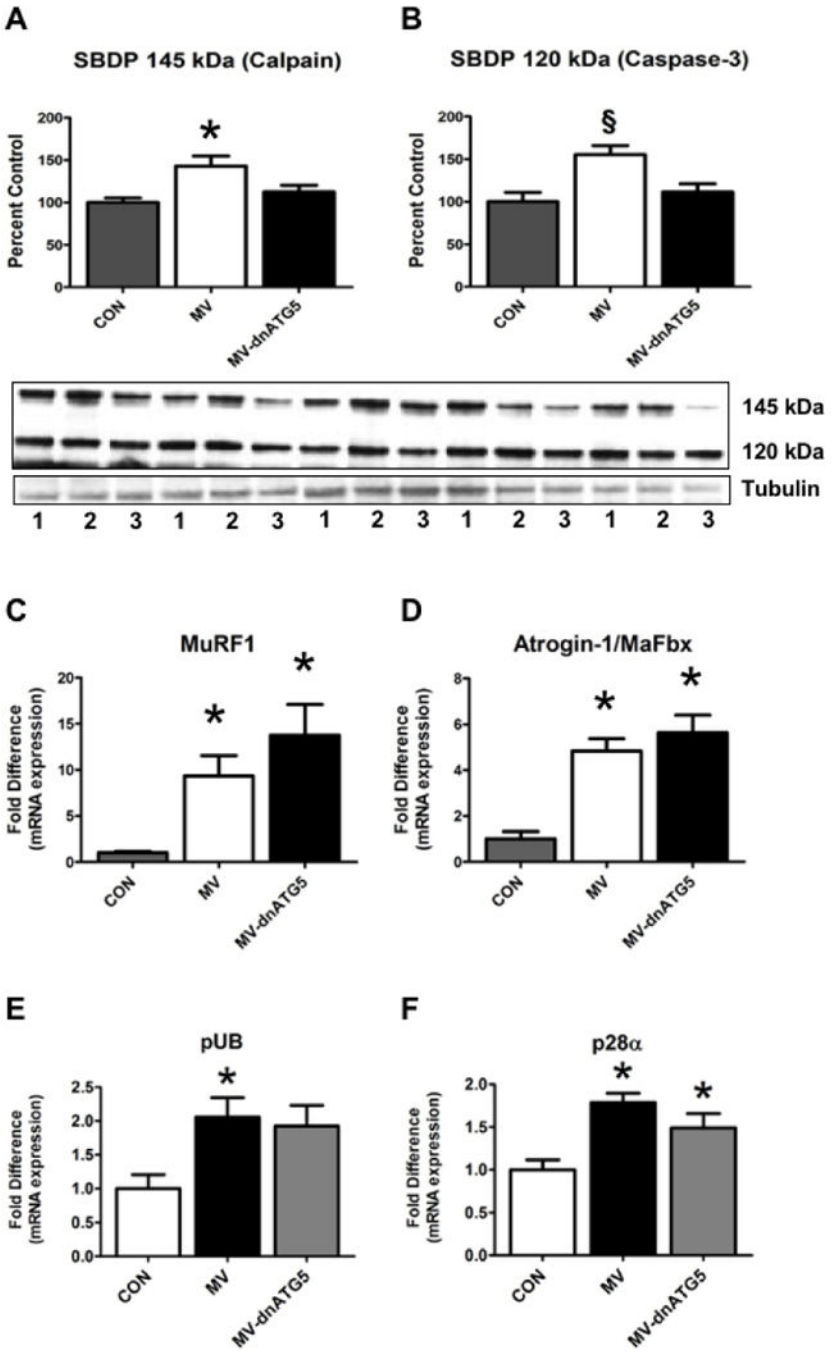

Figure 4.

Impact of MV on diaphragm markers of proteolysis. The spectrin breakdown product (SBDP) was assessed as a marker of **(A)** calpain and **(B)** caspase-3 activity. Representative western blot images are shown below the graph. 1 = CON; 2 = MV; 3 = MV-dnATG5. **(C)** MuRF1, **(D)** Atrogin-1/MaFbx, **(E)** pUB and **(F)** p28α mRNA expression were assessed as markers of proteasome-mediated proteolysis. Values are mean ± SEM. § Significantly different versus all groups ($p<0.05$). * Significantly different versus CON ($p<0.05$).

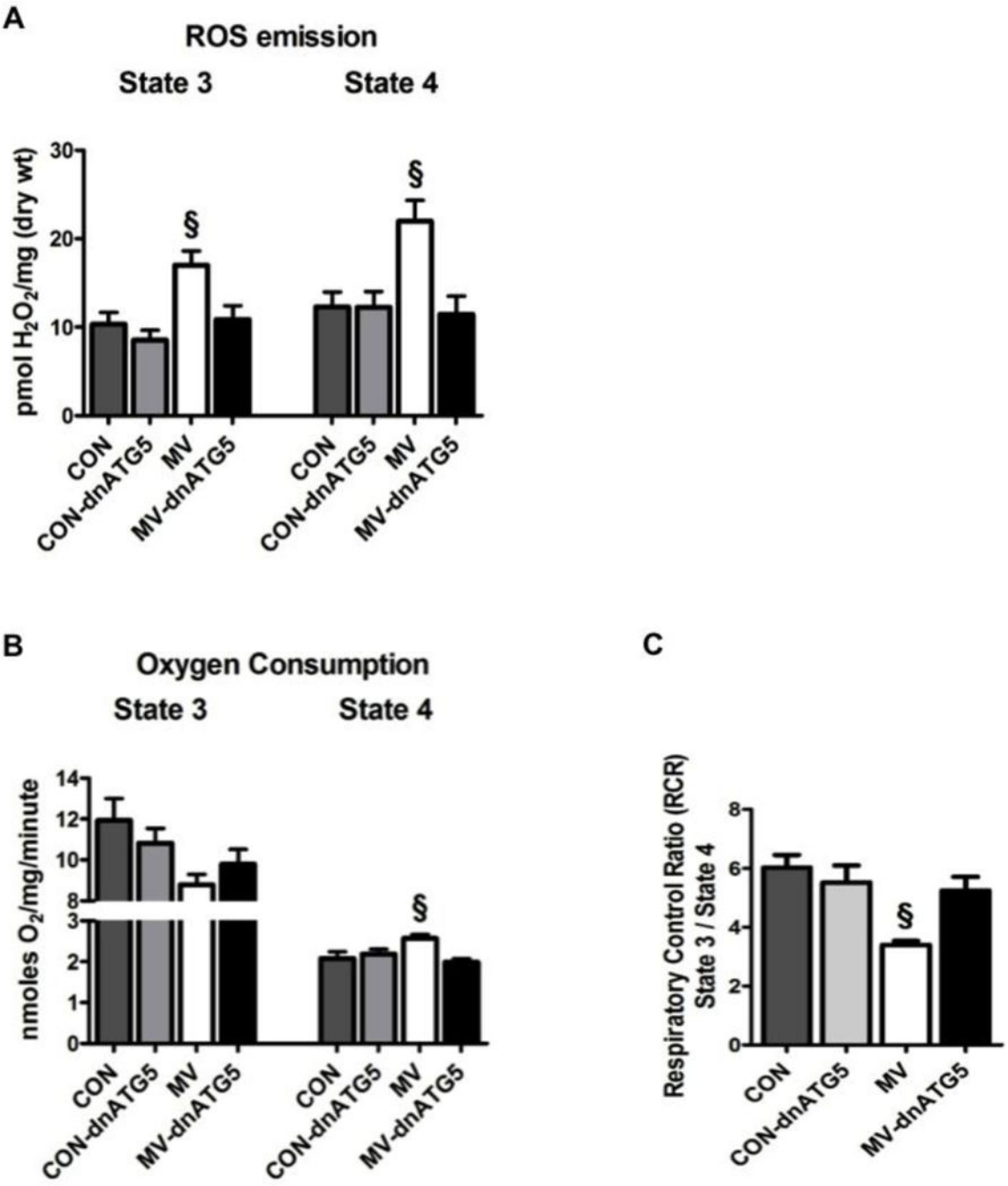

Figure 5.

Influence of MV on mitochondrial ROS emission and oxidative damage. **(A)** Diaphragm state 3 and state 4 mitochondrial ROS emission. **(B)** State 3 and state 4 mitochondrial oxygen consumption. **(C)** Mitochondrial respiratory control ratio (RCR). Values are mean ± SEM. § Significantly different versus all groups ($p<0.05$).

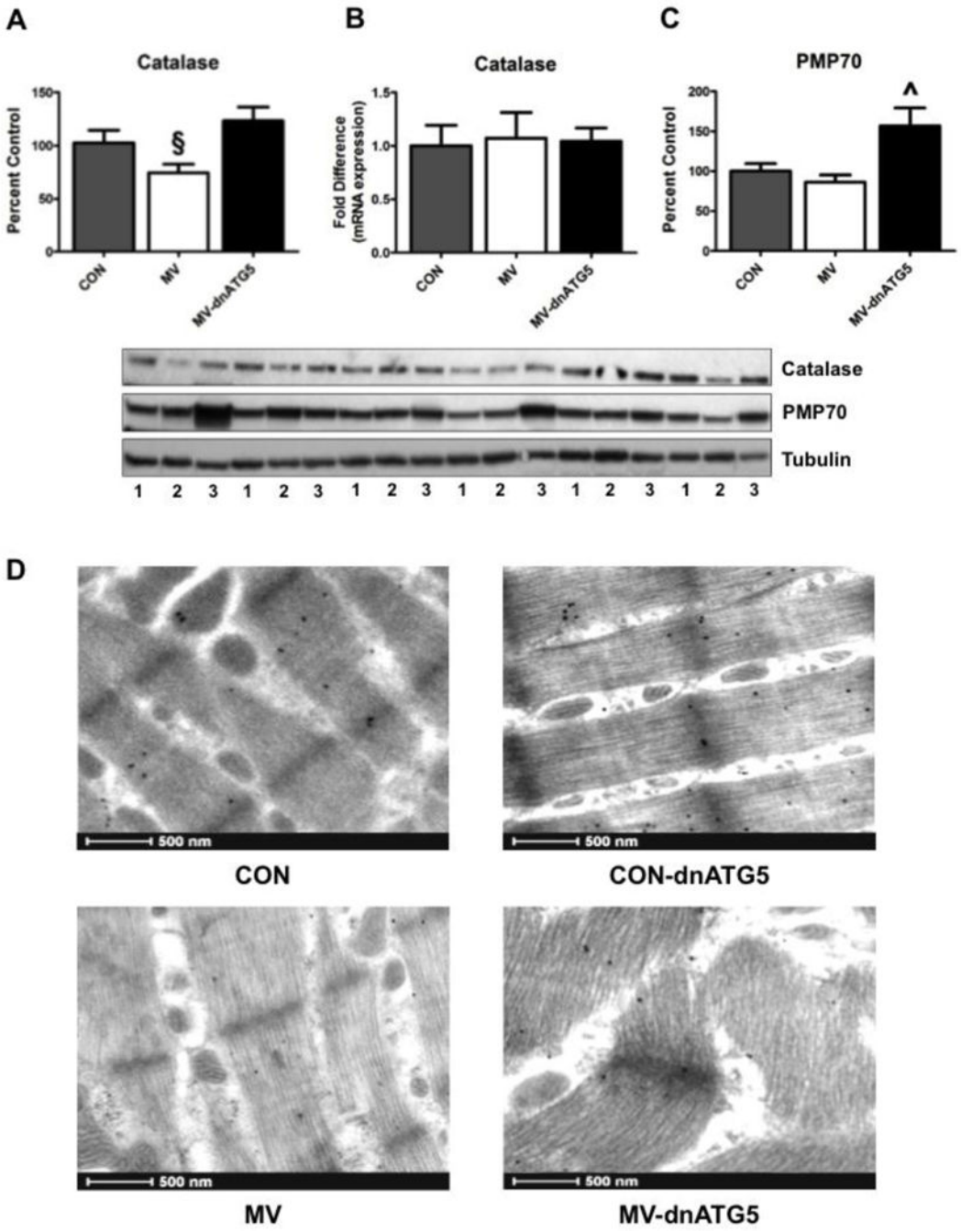

Figure 6.

Diaphragm catalase and peroxisome membrane protein expression. Catalase **(A)** catalase protein, **(B)** catalase mRNA **(C)** PMP70 protein expression and **(D)** immunogold labeling in the diaphragm. Black punctae within the diaphragm muscle images represent catalase expression. Representative western blot images for catalase and PMP70 are shown below the graph. 1 = CON; 2 = MV; 3 = MV-dnATG5. Values are mean ± SEM. § Significantly different versus all groups ($p<0.05$). ^ Significantly different versus CON and MV ($p<0.05$).

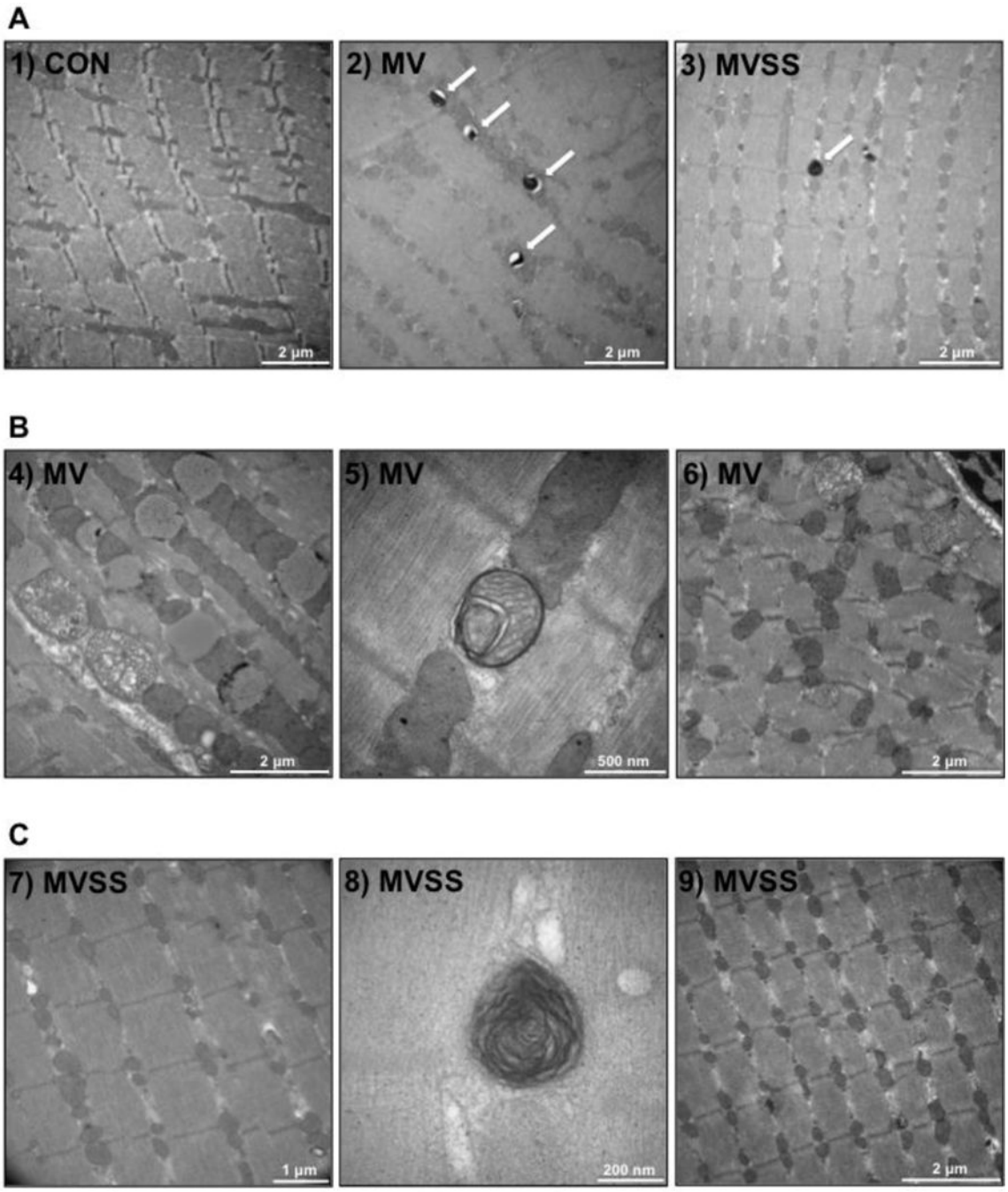

Figure 7.

Representative diaphragm muscle electron microscopy images for: **(A)** CON = control; non-ventilated, MV = mechanically ventilated for 12 hours, and MVSS = mechanically ventilated; SS-31 treatment. White arrows indicate autophagic vacuoles. **(B)** Images from MV diaphragms demonstrating rounded mitochondria with disrupted cristae structure; and **(C)** images from MVSS diaphragms demonstrating sparing of the mitochondrial structure.

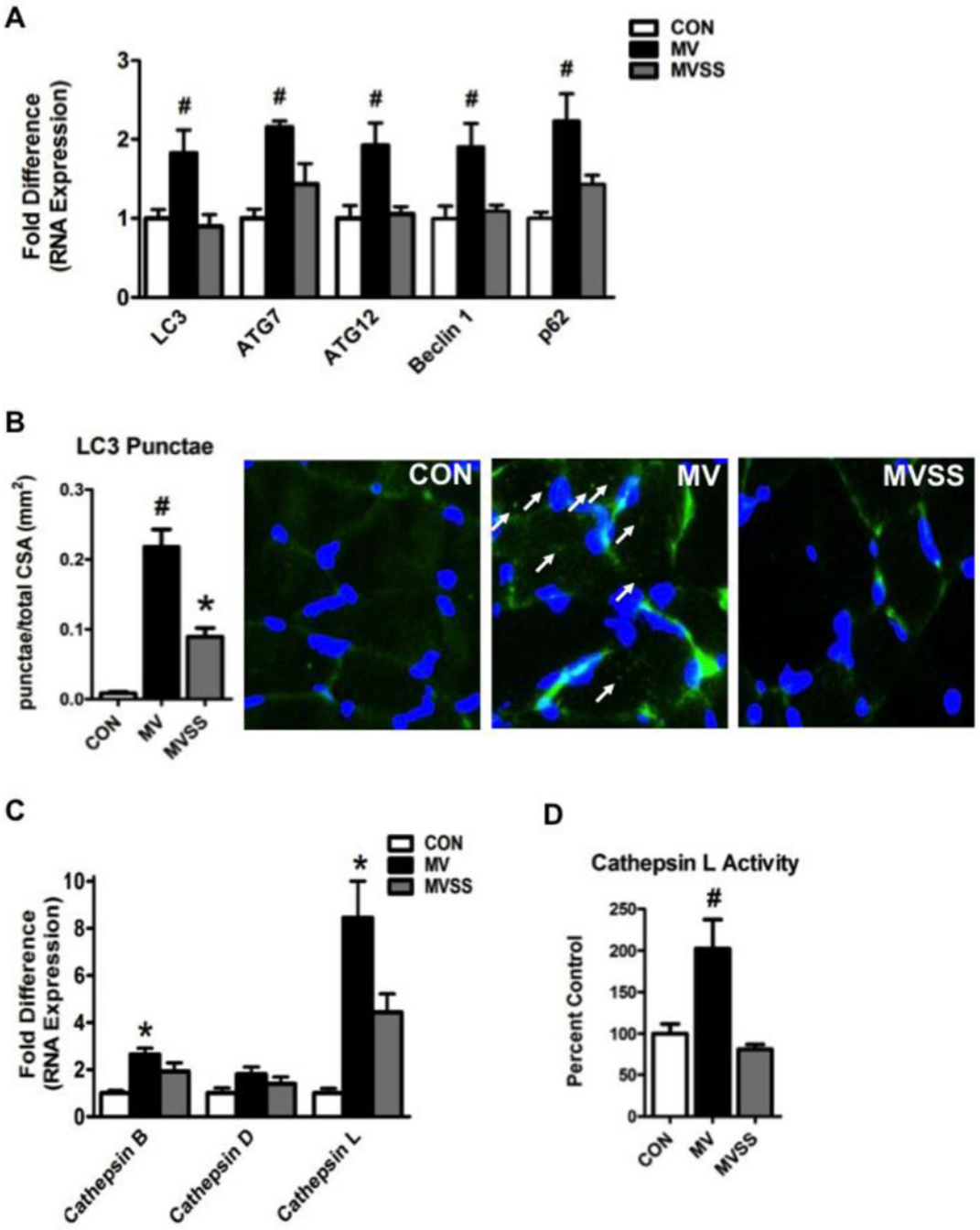

Figure 8.

Assessment of biomarkers of autophagy in mechanically ventilated animals treated with SS-31. **(A)** LC3, ATG7, ATG12, Beclin 1and p62 mRNA expression in the diaphragm. **(B)** Formation of LC3 punctae in the diaphragm. Representative images depicting the formation of LC3 punctae within the diaphragm muscle fibers are shown to the right of the graph. Sections were stained for myonuclei (blue) and LC3 (green). Green punctae denote LC3. Arrows denote punctae. **(C)** Cathepsin B, cathepsin D and cathepsin L mRNA expression and **(D)** cathepsin L activity were analyzed as markers of increased diaphragm protein

degradation by the lysosomal proteolytic system. Values are mean ± SEM. # Significantly different versus all groups ($p<0.05$). * Significantly different versus CON ($p<0.05$).

Table 1

Animal heart rates, systolic blood pressure, arterial blood gas tensions, and arterial pH at the completion of 12 hours of mechanical ventilation. Values are means ± SE. Note that no significant differences existed between the experimental groups in any of these physiological variables.

Physiological variable	MV	MV-dnATG5
Heart rate (beats/min)	359±12	367.2±6
Systolic blood pressure (mm/Hg)	104.3±4.7	105.8±3.3
Arterial PO_2 (mm/Hg)	78.3±1.9	82.3±2.6
Arterial PCO_2	39.4±2.3	34.1±1.9
Arterial pH	7.43±0.02	7.47±0.01